

IAA-PDC-15-04-04

MODELING MOMENTUM TRANSFER FROM THE DART SPACECRAFT IMPACT INTO THE  
MOON OF DIDYMOS

A.M. Stickle<sup>(1)\*</sup>, J.A. Atchison<sup>(1)</sup>, O.S. Barnouin<sup>(1)</sup>, A.F. Cheng<sup>(1)</sup>, C.M. Ernst<sup>(1)</sup>, Z. Fletcher<sup>(1)</sup>, D.C. Richardson<sup>(2)</sup>, and A.S. Rivkin<sup>(1)</sup>

<sup>(1)</sup>Johns Hopkins University Applied Physics Laboratory, 11100 Johns Hopkins Rd. Laurel MD 20723, USA, 240.228.3822, Angela.Stickle@jhuapl.edu

<sup>(2)</sup>Department of Astronomy, University of Maryland, College Park MD 20742, USA

**Keywords:** AIDA, DART Mission, Kinetic Impactor, Momentum Transfer, Impact Simulations

**Extended Abstract—**

**Introduction**

There are roughly 1000 near-Earth objects with sizes greater than 1 km, any of which would have civilization-wide consequences if they were to impact the Earth. Even smaller objects, such as that responsible for the 1908 Tunguska fireball, can devastate entire regions. Given sufficient notice, however, there are several notional mechanisms for deflecting these objects: “gravity tractors”, exploitation of Yarkovsky effects, and more active techniques such as nuclear weapons and kinetic impactors.

The Asteroid Impact and Deflection Assessment (AIDA) mission is a joint concept between NASA and ESA designed to test the effectiveness of a kinetic impactor. The mission is composed of two independent, but mutually supportive, components: the NASA-led Double Asteroid Redirect Test (DART), and the ESA-led Asteroid Impact Monitoring (AIM) mission. The spacecraft will be sent to the near-Earth binary asteroid 65803 Didymos, which makes unusually close approaches to Earth in 2022 and 2024. These close approaches make it an ideal target for a kinetic impactor asteroid deflection demonstration, as it will be easily observable from Earth.

The DART spacecraft, nominally  $\sim 2 \text{ m}^3$  and 300 kg, will act as a kinetic impactor experiment and will impact the moon ( $\sim 150 \text{ m}$  diameter) of the binary system at 6.25 km/s. The deflection of the moon will then be determined by the orbiting AIM spacecraft and from ground-based observations by measuring the change in the moon’s orbital period. The spacecraft must impact the target asteroid in a direction that maximizes the imparted orbital period change. This drives the arrival relative velocity into the moon’s orbit plane relative to Didymos. In addition, the lighting must be favorable for approach optical navigation to ensure that the target can be identified and differentiated from the primary asteroid. In the 2019 to 2022 timeframe, four launch periods offer direct chemical trajectories that meet these requirements, each leading to impact on 01 October 2022. The transfer trajectories depart with high declination of launch asymptotes, which

provide the required change in inclination between Earth and Didymos. The trajectories impact the asteroid near its close approach with Earth, below the ecliptic plane. This orientation requires relatively low launch energy and enables low cost launch vehicle options.

In support of this mission concept, a modeling study was performed to determine the expected momentum transfer to the moon following impact. The combination of CTH hydrocode models, analytical scaling predictions, and *N*-body *pkdgrav* simulations helps to constrain the expected results of the kinetic impactor experiment, including crater size, ejecta mass, momentum transfer, and trajectory deflection following impact. Because the physical properties of the target are not well constrained, these modeling studies cover a range of possible material properties.

**Modeling Studies**

*Analytical Scaling Predictions* – Crater scaling rules [e.g., 1-4] can be used to estimate the amount of ejecta expected to escape both the moon and the binary system following impact as well as the final crater size. The most likely scenario for the moon’s material properties is that of a highly porous rock that possesses some shear and compressive strength, but little tensile strength. This is because the moon of a small binary asteroid is likely the result of re-accreting regolith that was shed by the parent binary to produce a loosely bound, highly porous moon [e.g., 5]; the material resistance to deformation will then mostly depend on the confining pressure from the self-gravity holding the aggregate together. For the case of the DART impact, in order for the cratering process on Didymos’ moon to be gravity dominated, the effective strength of the moon would have to be  $\sim 4 \text{ Pa}$  [1,3]. This is probably unreasonably low and the DART impact into the moon of Didymos is likely to be a strength-dominated event. We consider a range of possible material strength values for the moon between 0 and 18 MPa (representing unconsolidated, strengthless sand or hard rock, respectively). Gravity-dominated crater scaling rules

provide upper-limits for the calculations. In these models, we do not consider porosity.

For the chosen range of strength values and scaling parameters from [1], the DART impact would form a crater between 8 and 114 m in diameter, for hard rock and strengthless sand, respectively. These same craters would have a cumulative mass of escaping ejecta of  $\sim 10^4$  and  $\sim 10^6$  kg. The most likely range of scenarios (i.e., strength values and scaling parameters), however, result in a final crater size between 8 and 17 m and a cumulative mass of escaping ejecta between  $\sim 10^4$  and  $10^5$  kg, roughly 0.01-0.03% of the moon's mass.

Using the scaling relationships in [1-4] and a correction for ejecta retained by the target asteroid [1], we also computed the momentum transfer ( $\beta$ ) and change in velocity ( $\Delta v$ ) for four target types: a strong rock, a weakly cemented rock, a highly porous weak rock, and a cohesionless sand-like surface. This method expands on results above by including the effects of porous material. Results of these calculations for the different target types are shown in Table 1. Three cases included here are likely too strong (competent rock), too dense (weak rock), or too unrealistic (cohesionless), however they do help place constraints and bounds on the expected  $\Delta v$  and  $\beta$  generated by the DART impact.

**Table 1:** Velocity imparted to a target asteroid after impact by DART for different composition targets, including the effects of porosity

| Material            | Asteroid density (kg/m <sup>3</sup> ) | Effective strength (kPa) | $\beta$ | $\Delta v$ (mm/s) |
|---------------------|---------------------------------------|--------------------------|---------|-------------------|
| Competent rock      | 3000                                  | 300                      | 5.00    | 1.76              |
| Weak rock           | 2600                                  | 200                      | 1.31    | 0.53              |
| Highly porous, weak | 1000                                  | 2                        | 1.49    | 3.16              |
| Cohesionless sand   | 1700                                  | 0                        | 2.05    | 4.26              |

*Impact Simulations* - To better understand the large parameter space, simulations of the DART impact were performed using the CTH hydrocode from Sandia National Laboratories [6]. Because the physical properties of the Didymos system are not well known, we examined a variety of target properties (e.g., material strength and porosity) and impact scenarios to constrain the expected results of the DART impact. Mission design constraints provide an impact velocity and a likely impact location with respect to the center of figure (COF) of the moon. However, impact angle (whether due to an inclined trajectory or to local surface topography) is not well constrained. To better inform mission design, we examined the effects of impact location (e.g., where DART impacts with respect to the center of figure), and impact angle on crater size and shape, and momentum

transfer following impact using both 2D and 3D models with a variety of equations of state, strength models, and adaptive mesh refinement (AMR) [7].

Final crater geometry can be examined for these simple, small craters to determine how it may change as a function of target properties (e.g., Fig. 1). Each scenario shown here results in a slightly different crater shape and size. The three fully dense models all have similar-sized final craters, but the model with an initial density of 1.7 g/cm<sup>3</sup> (i.e., higher porosity) forms a much smaller crater with steeper walls than models without porosity. As the impact gets farther from the COF of the target, the effective impact angle becomes more oblique, resulting in an asymmetric crater. This will have important implications for the ejecta trajectories, and thus the momentum transfer to the moon. For increasingly oblique impacts, ejecta are concentrated downrange [e.g., 8] (here, the x direction), which lessens the thrust from the ejecta in the orbit direction.

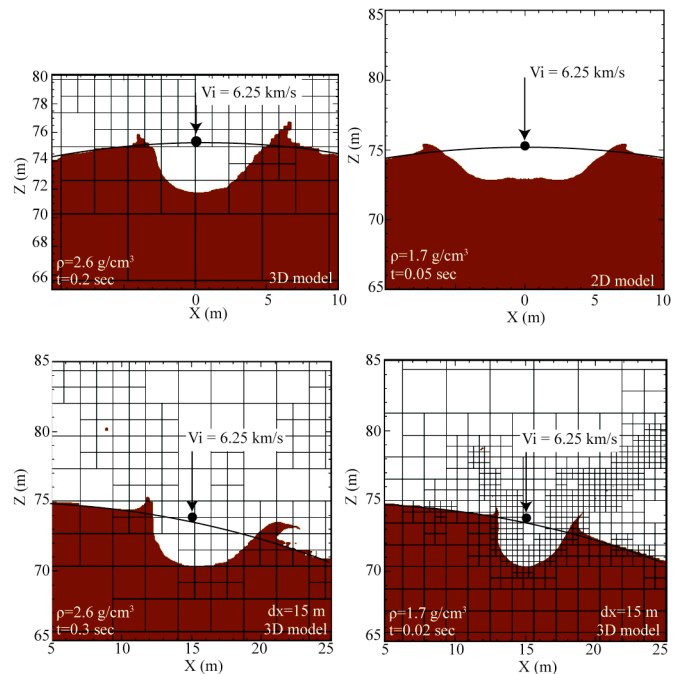


**Fig. 1.** Final crater sizes for differing initial impact scenarios. All models were run in a rectangular coordinate system. Craters finish forming more quickly in models including porosity (bottom right), and they are smaller than in the fully dense case (bottom left). The grid lines show the effect of adaptive mesh refinement (AMR) on the resolution, with higher resolution around the ejecta. The initial impact location, projectile size, and velocity are shown for reference. The black arc represents the original surface of the moon, for reference.

For “realistic” material properties (sand or weak/soft rock) the analytical models predicted crater diameters between 8 and 17 m. Specifically, the models of weak rock, with yield strength of 7.6 MPa, predict crater

diameters of 12 m, while “sand” with yield strength of 1 MPa predict a crater diameter of 8 m. For equivalent impacts (90°, through the COF), the range predicted by these CTH simulations is 6–15 m, a difference of 12–25% from the analytical predictions.

The momentum transferred to the asteroid following impact is parameterized here by  $\beta$ , which represents the momentum enhancement of the moon. This enhancement comes from the addition of the initial spacecraft momentum and the ejecta excavated during crater formation. To calculate  $\beta$  from the CTH simulations, the target (Didymos’s moon, represented here as a 150 m spherical object) was seeded with 1000 Lagrangian tracer particles to track the velocity and state of the material (e.g., temperature, pressure, density) as a function of time after impact. In the simulations, the moon is initially at rest, thus any velocity recorded by the tracers after impact can be used to calculate the motion of the body after impact. Assuming a rigid body (thus momentum is equal to the tracer velocity multiplied by the mass of the moon), the resultant momentum transfer of the moon,  $\beta$ , was then calculated by:

$$\beta = 1 + \frac{P_{\text{moon}}}{P_{\text{spacecraft}}}$$

where  $p_{\text{moon}}$  is the momentum of the moon following impact ( $v_z^{\text{avg}} * m_{\text{moon}}$ ), and  $p_{\text{spacecraft}}$  is the initial momentum of the spacecraft.

**Table 2:** CTH results for the change in velocity and momentum transfer to the moon following the DART impact. Impact trajectories were through the COF or offset to test effects of changing impact location/parameters.

| Target and impact parameter | $\Delta v$ COF (mm/s) | $\beta$ from COF vel ( $V_z \text{COF} * m$ ) |
|-----------------------------|-----------------------|---|
| Competent rock, COF         | 1.47                  | 3.8   |
| Competent rock, dx=15 m     | 2.24                  | 5.4   |
| Competent rock, dx=30 m     | 2.29                  | 5.5   |
| COF, porous                 | 0.07                  | 1.08  |
| dx=15m, porous              | 0.06                  | 1   |

Preliminary results of momentum transfer from the 3-D CTH models for a fully competent, strong (yield strength of 200 MPa) moon generally agree with predictions from analytical studies. For fully dense, competent, strong rocks, we calculate values for  $\beta$  between approximately 3.8 and 5.5, with an imparted  $\Delta v$  of 1.47–2.29 mm/s to the moon for impacts at various distances ( $dx$ ) from the

COF ( $dx=0-30$  m) (Table 2). These  $\beta$  values compare favorably with the analytical solutions shown in Table 1 for the competent rock, indicating that the impact location with respect to the COF will affect the momentum transfer in the direction of interest (in the ecliptic plane, along the direction of motion, here assumed to be the z-direction). When porosity is added to the numerical models, the calculated  $\beta$  values drop below those estimated for the porous analytical case, and can be as small as  $\beta \sim 1$ .

*N-body simulations* - Following impact, *pkdgrav* [5] simulations of the system evolution track changes in the orbital period of the moon and examine the effects of the shapes of Didymos and its moon on the deflection. *Pkdgrav* permits consideration of more complex geometries than is possible with the analytical solutions. This includes investigating changes in the velocity of the moon out of its orbit plane, and the effects of a realistic primary shape on the moon’s orbital dynamics. These simulations indicate that the shapes of the bodies can influence the trajectory deflection of the moon.

The resultant  $\Delta v$  calculated in the previous section is used to evaluate the consequences on the subsequent orbital evolution of Didymos’s moon. Initially, two simple models of the Didymos binary system are considered: a two-particle system and an aggregate primary. The moon of Didymos is assumed to be a 150 m diameter sphere in all cases, located at 1.095 km from the center of the 0.8-km-diameter primary. The baseline case is for a moon that has no eccentricity or inclination ( $e, i = 0$ ). The primary was assigned a rotation rate of 2.6 h, and the secondary an orbital period of 11.9 h [9]. No small body forces such as YORP or Yarkovsky are modeled. These forces could influence the dynamics of the secondary, but over much longer time scales than the time expected for both AIM and Earth-based observations following DART’s impact; thus, they are not considered here.

The  $\Delta v$  explored includes adjustment in the secondary’s velocity both in and opposite to the secondary’s orbit direction, and at some angle to the orbit direction both in and out of the binary’s orbit plane. Fig. 2 shows some examples of the results and illustrates that, for most impact conditions considered in the two-particle system, changes in orbital dynamics of the moon of Didymos can be observed easily from both AIM and Earth-based facilities. For the three cases shown in Figure 2, the DART impact causes a shift in the moon’s orbital period of 8.8 minutes (Fig. 2, middle and bottom) to 10.1 minutes (Fig. 2 top). These simulations indicate that impacts in-plane and in the orbit direction are best for Earth-based measurement, but that off-axis impacts still result in noticeable period changes. Preliminary investigation making use of a more realistic primary aggregate appear to enhance some of the changes in the orbital evolution of the secondary, with the most noticeable changes in the orbital eccentricity.

References

- [1] Holsapple, K.A. and K.R. Housen, 2012. Momentum transfer in asteroid impacts I. Theory and scaling, *Icarus* 221, p. 875-887.
- [2] Housen, K.R., Schmidt, R.M., Holsapple, K.A., 1983. Crater ejecta scaling laws: Fundamental forms based on dimensional analysis, *Journal of Geophysical Research* 88, p. 2485–2499.
- [3] Richardson, J. E., Melosh, H.J., Lisse, C. M., and Carcich, B., 2007, A ballistics analysis of the Deep Impact ejecta plume: Determining Comet Tempel 1's gravity, mass, and density, *Icarus*, 190(2), 357–390, doi:10.1016/j.icarus.2007.08.001.
- [4] Housen, K.R., Holsapple, K.A., 2011. Ejecta from impact craters, *Icarus* 211, p. 856–875.
- [5] Walsh, K.J., Richardson, D.C. & Michel, P., 2008. Rotational breakup as the origin of small binary asteroids. *Nature*, 454(7), pp.188–191.
- [6] McGlaun, J.M, Thompson, S.L. and Elrick, M.G., 1990. CTH: A three-dimensional shock wave physics code, *International Journal of Impact Engineering*, 10(1-4), p. 351-360.
- [7] Crawford, D.A. et al. 2006. Adaptive Mesh Refinement in the CTH Shock Physics Hydrocode, *The Russian Journal of Physical Chemistry B*, 25:9, p. 85-90.
- [8] Anderson, J.L.B, Schultz, P.H, Heineck, J.T., 2003. Asymmetry of ejecta flow during oblique impacts using three-dimensional particle image velocimetry, *Journal of Geophysical Research* 108, E8, doi: 10.1029/2003JE002075
- [9] JPL Small-Body Database Browser on 65803 Didymos

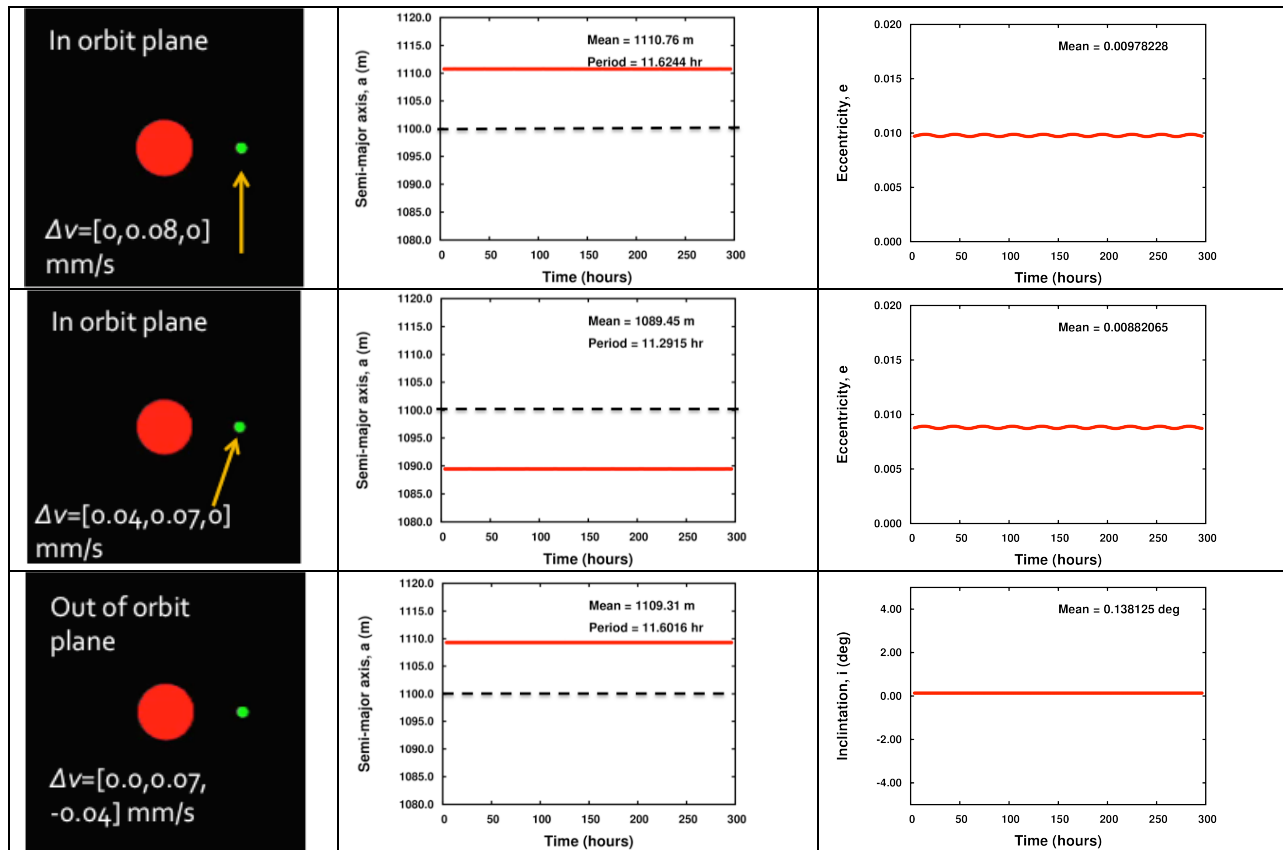


**Figure 2.** Some examples of consequences of  $\Delta v$  imparted by DART to the moon of Didymos. (top) impact into the moon in it's orbital plane in the parallel to orbital velocity; this impact scenario causes a period change of 10.1 minutes. (middle) Impact into the moon in it's orbital plane but oblique to orbital velocity; this impact scenario causes a period change of 8.8 minutes. (bottom) Impact out of the moon's orbital plane; this impact scenario causes a period change of 8.8 minutes.